

See discussions, stats, and author profiles for this publication at: <https://www.researchgate.net/publication/271979050>

Effect of Annealing on Structure and Mechanical Behavior of an AA2139 Alloy

Article in *Materials Science Forum* · May 2014

DOI: 10.4028/www.scientific.net/MSF.783-786.258

CITATIONS

2

READS

21

4 authors, including:



[Daria Zhemchuzhnikova](#)

Belgorod State University

19 PUBLICATIONS 54 CITATIONS

[SEE PROFILE](#)



[Marat Gazizov](#)

Belgorod State University

22 PUBLICATIONS 69 CITATIONS

[SEE PROFILE](#)



[Rustam Kaibyshev](#)

Belgorod State University

417 PUBLICATIONS 4,367 CITATIONS

[SEE PROFILE](#)

Some of the authors of this publication are also working on these related projects:



Most of our researchers are concentrating on Dynamic Transformation. We are now looking into the behavior of Ti alloys. [View project](#)



Development of high-Mn austenitic steels with improved fatigue properties [View project](#)

All content following this page was uploaded by [Rustam Kaibyshev](#) on 31 March 2016.

The user has requested enhancement of the downloaded file. All in-text references [underlined in blue](#) are added to the original document and are linked to publications on ResearchGate, letting you access and read them immediately.

Effect of Annealing on Structure and Mechanical behavior of an AA2139 Alloy

Damir Tagirov¹, Daria Zhemchuzhnikova², Marat Gazizov³,
Rustam Kaibyshev⁴

Belgorod State University, Pobeda 85, Belgorod 308015, Russia

¹ tagirov@bsu.edu.ru, ² zhemchuzhnikova@bsu.edu.ru, ³ gazizov@bsu.edu.ru,
⁴ rustam_kaibyshev@bsu.edu.ru

Keywords: aluminum alloy, precipitation, high temperature deformation, mechanical properties, microstructure, fracture

Abstract. An AA2139 alloy with a chemical composition of Al–4.35Cu–0.46%Mg–0.63Ag–0.36Mn–0.12Ti (in wt.%) and an initial grain size of about 155 μm was subjected to annealing at 430°C for 3 h followed by furnace cooling. This treatment resulted in the formation of a dispersion of coarse particles having essentially plate-like shape. The over-aged alloy exhibits lower flow stress and high ductility in comparison with initial material in the temperature interval 20–450°C. Examination of microstructural evolution during high-temperature deformation showed localization of plastic flow in vicinity of coarse particles. Over-aging leads to transition from ductile-brittle fracture to ductile and very homogeneous ductile fracture at room temperature.

Introduction

Currently, there is a considerable interest in developing technologies for the manufacturing of critical components from novel Al–Cu–Mg–Ag alloys in aviation industry. These alloys exhibit excellent mechanical properties including high strength, superior creep resistance and fracture toughness, fatigue life due to the formation of the fine and uniform dispersion of the Ω -phase with plate-like shape on the $\{111\}_\alpha$ planes of the aluminum matrix [1,2]. Numerous works were dealt with examination of the precipitation behavior and mechanical properties of these alloys [2-5]. However, the effect of precipitates produced by over-aging on workability of these alloys was considered in very limited number of studies [6] despite its importance for cold rolling and forging, where metal can be shaped through plastic deformation without introducing any defect. Optimization of a dispersion of secondary phase by over-aging may significantly enhance workability of high strength aluminum alloys [7]. In addition, the deformation conditions have great effects on the mechanical properties of Al–Cu–Mg–Ag alloys [3,8]. The aim of this paper is to report the effect of over-aging on the mechanical behavior and microstructural evolution of an Al–Cu–Mg–Ag alloy during tensile test at temperatures ranging from 20 to 450°C.

Experimental Procedure

The AA2139 alloy (Al–4.35Cu–0.46%Mg–0.63Ag–0.36Mn–0.12Ti (in wt.%) was examined. This alloy was produced by semi-continuous casting followed by homogenization annealing at 510°C for 24 hours. This material will denote as initial or as-cast alloy. Rods with dimensions of 20 mm \times 20 mm \times 100 mm were machined from the central part of ingot. These machined rods were subjected to pressing at 400°C up to a total strain of ~ 2 . Next, the AA2139 alloy was solution treated at 510°C for 1h and subsequently water quenched. Over-aging was carried out at 430°C for 3h. This alloy is denoted as over-aged one.

Tensile tests were carried out using an Instron 5882 testing machine in the temperature interval 20–450°C at strain rates ranging from 2.8×10^{-4} to $2.8 \times 10^{-1} \text{ s}^{-1}$. The each sample was held at the testing temperature for about 10 min in order to reach thermal equilibrium. The values of the strain rate sensitivity (m) were determined by strain-rate-jump tests [9].

The details of sample preparation for structural characterization by transmission electron microscopy (TEM), scanning electron microscopy (SEM) and phase analysis, techniques used for estimation of the volume fraction of the secondary phase particles, the average dislocation density were described in previous works [6] in details. TEM studies were performed on fractured samples which were at an initial strain rate of $5.6 \times 10^{-3} \text{ s}^{-1}$ at different temperatures.

Results and Discussion

Microstructures before and after over-aging. Typical TEM images of the AA2139 alloy are shown in Fig. 1. The as-cast alloy contains fine globular and rod-shaped dispersoids, which relatively uniformly distributed within grains. The average particles sizes are ~ 360 and ~ 100 nm in longitudinal and transverse directions, respectively, they volume fraction and average inter-particle spacing are $\sim 5\%$ and $\sim 0.7 \mu\text{m}$, respectively (Fig. 1a). Annealing at 430°C led to coarsening initial particles by a factor of about 1.5 to the dimensions of ~ 550 and ~ 150 nm, respectively (Fig. 1b). The volume fraction of particles after over-aging slightly increases to $\sim 7\%$. The inter-particle spacing increases to $1.1 \mu\text{m}$ (Fig. 1b). These particles retain within aluminium matrix.

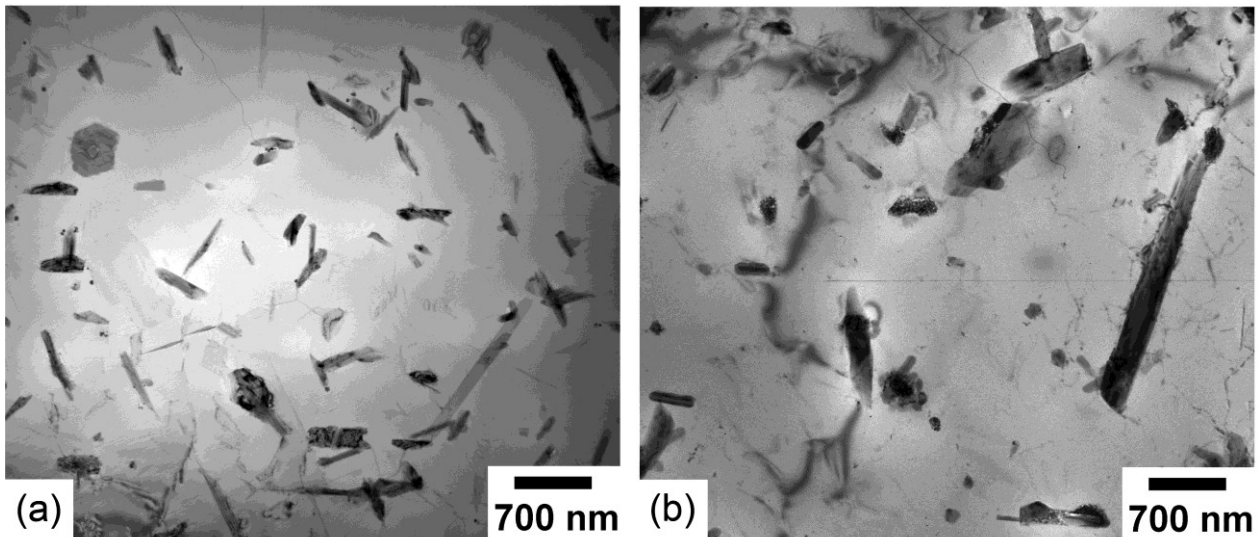


Fig. 1. Microstructures of the AA2139 alloy: (a) as-cast and (b) over-aged states.

Mechanical behavior. The typical engineering stress vs. strain curves for the AA2139 alloy before and after over-aging are shown in Figure 2 at an initial strain rate of $5.6 \times 10^{-3} \text{ s}^{-1}$ in the temperature interval $20\text{-}450^\circ\text{C}$. It is seen that over-aging increases elongation-to-failure to 30% in the temperature interval $20\text{-}200^\circ\text{C}$ as compared with the as-cast alloy, while at higher temperatures the ductilities of the AA2139 alloy in the two conditions are nearly the same. Moreover, over-aging decreases flow stress significantly. Shape of the $\sigma\text{-}\epsilon$ curves is essentially the same for both conditions. A significant initial strain hardening occurs in the temperature interval $20\text{-}200^\circ\text{C}$. Over-aging decreases the strain hardening coefficient and increases peak strain. At ambient temperature, the initial alloy fractures at the stress peak, while in the over-aged alloy after reaching a maximum stress, the flow stress continuously decreases until fracture (Fig. 2). Peak strain decreases with increasing temperature. The over-aged AA2139 alloy shows a weak evidence for jerky flow that is attributed to dynamic strain aging (DSA) [10].

In the temperature interval $300\text{-}450^\circ\text{C}$ a peak stress is attained after a very short transient stage of plastic deformation (Fig. 2). Flow stress continuously decreases until fracture (Fig. 2). In the temperature interval $400\text{-}450^\circ\text{C}$, an apparent steady-state flow could be distinguished before

fracturing (Fig. 2) and the samples exhibit high ductilities (~120-140%). At 450°C, flow stresses of the both states of the AA2139 alloy become nearly the same.

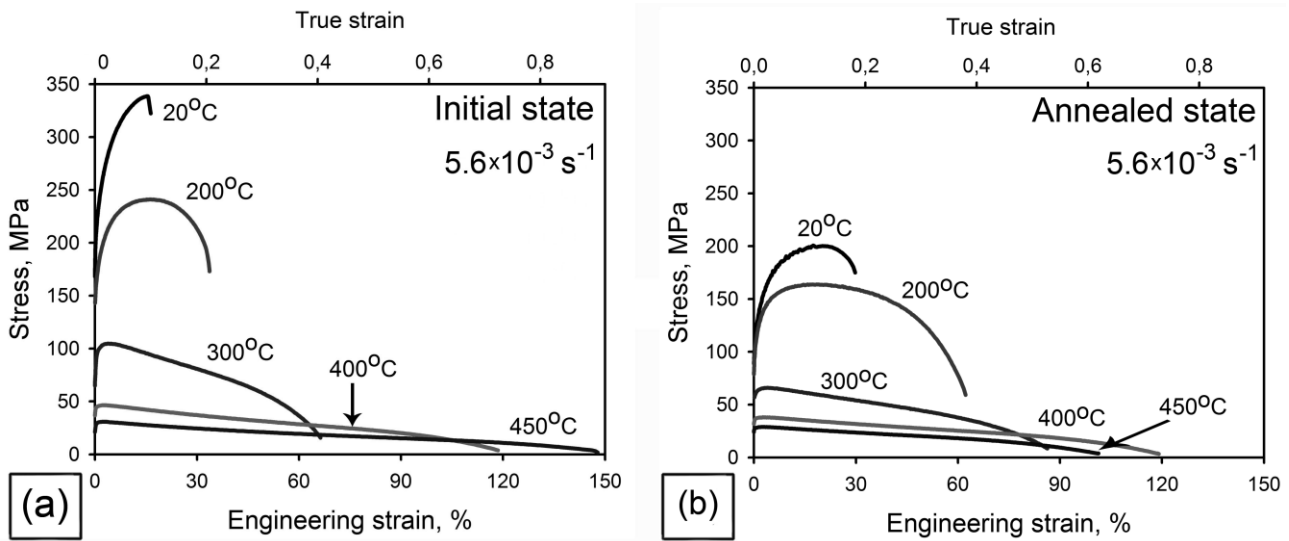


Fig. 2. Effect of temperature on the stress- strain curves for the AA2139 in initial and over-aged conditions.

Effect of strain rate on the σ - ϵ curves and variations of the coefficient of strain rate sensitivity, m , with strain rate are shown in Fig.3 for strain rates ranging from $\sim 10^{-4}$ to $\sim 10^{-1}$ s^{-1} in the temperature interval 400-450°C for the over-aged alloy. The main feature of high-temperature mechanical behavior is extensive strain softening after peak that can lead to plastic instability and low ductilities. Low value of m could not prevent extensive necking [9]. However, softening is apparent. Re-plotting tension curves to true stress – true strain form revealed that there is steady state flow at these conditions (Fig.3). Therefore, a relatively high ductility of 120% was achieved due to combination of steady-state flow with low m values (Fig.3). Increasing strain rate or decreasing temperature result in increased the peak stress (Fig. 3a,b). Temperature and strain rates affect insignificantly the elongation-to-failure (Fig.3a,b). The highest m values of ~ 0.16 and ~ 0.17 for the 400°C and 450°C are observed at strain rate of $\sim 3.3 \times 10^{-3}$ and $\sim \times 10^{-3}$ s^{-1} , respectively (Fig. 3c).

At ambient temperature, tension induced a high density of lattice dislocations ($\rho \sim 3 \times 10^{14} m^{-2}$) (Fig.4a). The accumulation of lattice dislocation occurs in vicinity of coarse plates which play a role of obstacles for dislocation glide (Fig. 4a). Increasing temperature leads to a significant reduction in the dislocation density ($\rho \sim 10^{14} m^{-2}$), most of dislocation arrange to subgrains (Fig. 4b).

Fractography. Fractographs of the fractured specimens tensioned at 20°C are shown in Fig. 5. At room temperature, the as-cast alloy exhibits brittle-ductile fracture; deep, coarse dimples with conical shape alternate with very fine shallow dimples and cleavage zones (Fig.5a) The fracture surfaces of the initial alloy is inhomogeneous, the numerous brittle cracking are visible at the bottom of large dimples (Fig. 5a). However, ductile transgranular fracture is in dominant (Fig. 5a). [12]. The fracture is initiated by the separation of secondary phase particles, which are typically present at the bottom of dimples that leads to the appearance of deep dimples (Fig. 5b). The nucleation sites are few and widely spaced. No significant microvoid coalescence takes place. Propagation of cracks originated from these deep dimples requires considerable plastic deformation (Fig.5b).

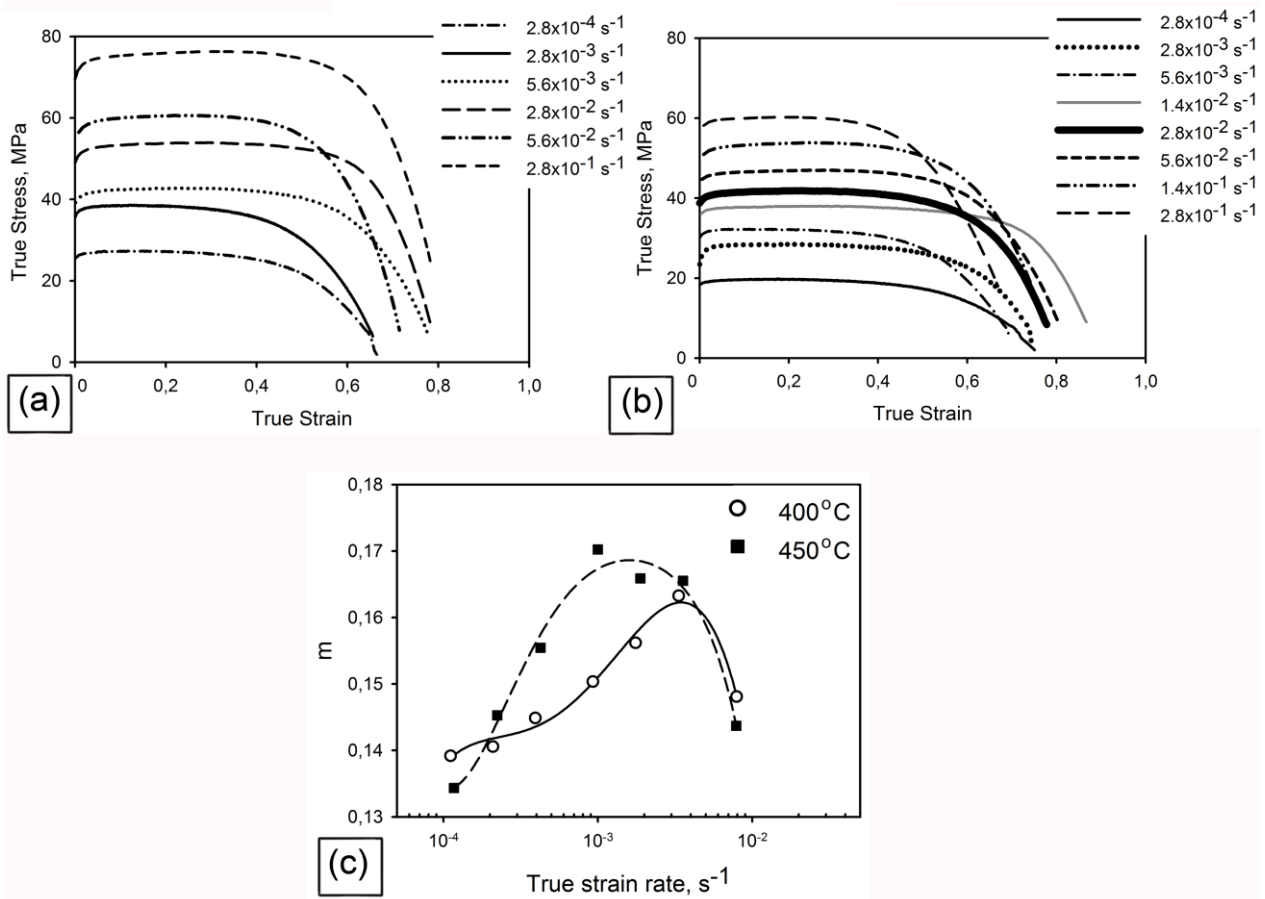


Fig. 3. Effect of strain rate on the stress-strain curves (a,b) and the coefficient of strain rate sensitivity, m , (c) for the annealed AA239 alloy .

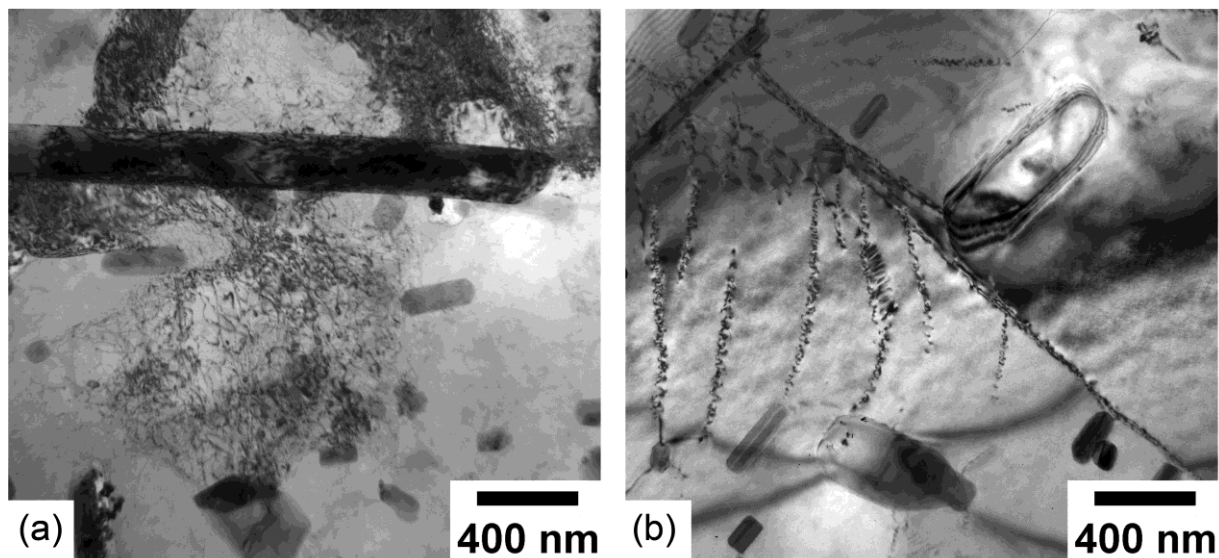


Fig. 4. Microstructure of the annealed AA239 alloy deformed at (a) room temperature and (b) 450°C . $\dot{\epsilon} = 5.6 \times 10^{-3} \text{ s}^{-1}$.

The over-aged alloy demonstrates the uniform fracture surfaces (Fig.5a',b'); ductile transgranular fracture occurs takes place. The observation of numerous small deep dimples is indicative for activation of a number of nucleating sites. As shown in Fig. 5b', the particles of secondary phases are also observed on the bottom of these dimples. Therefore, coarsening and increasing the volume fraction of particles due to over-aging led to the formation of many nucleation sites of the microvoids. Their growth to large sizes before coalescing is hindered.

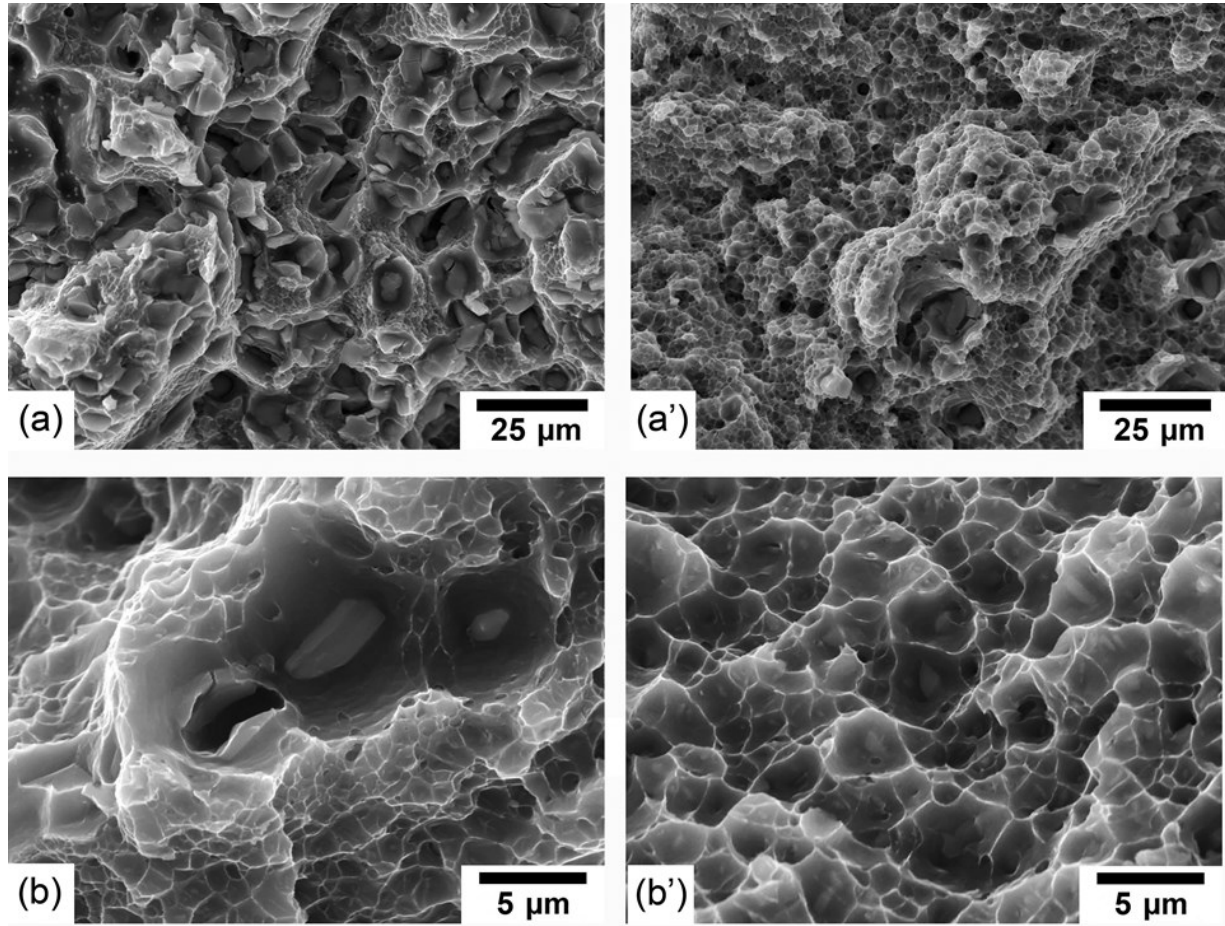


Fig. 5. SEM of the tensile fracture surface of the AA2139 alloy: (a, b) as-cast state (a', b') over-aged state. T=20°C.

Thus, over-aging of the AA2139 alloy decreases significantly flow stress and provides ductile fracture at room temperature despite the fact the secondary phases retain plate-like shape and their dimensions are less than 1 μm . Workability of over-aged AA2139 alloy is sufficient for cold rolling of thin sheets and the forming of structural components with complicated shape at $\sim 400^\circ\text{C}$.

Summary

Over-aging of the AA2139 alloy at 430°C for 3 h led to coarsening initial particles by a factor of about 1.5, that improves ductility to 30% and provides -40% decrease in the peak stress over the entire temperature interval 20- 450°C . It was shown, that highest tensile elongations of $\sim 120\%$ the alloy exhibits in the temperature interval 400- 450°C and the strain rate affect insignificantly the elongation-to-failure. Examination of microstructural evolution during tensile deformation showed extensive increase in dislocation density and localization of plastic flow in vicinity of coarse particles.

Acknowledgements

This study was supported by grant No. OK-539/0402-13. The main results were obtained by using equipment of Joint Research Centre, Belgorod State University.

References

- [1] Y.C. Chang, J.M. Howe, Composition and stability of Ω phase in an Al-Cu-Mg-Ag alloy, *Metall. Trans. A* 24A (1993) 1461-1470.
- [2] D. Bakavos, P.B. Prangnell, B.Bes, F.Eberl, The effect of silver on microstructural evolution in two 2xxx series Al-alloys with a high Cu:Mg ratio during ageing to a T8 temper, *Mater.Sci.Eng. A* 491 (2008) 214–223.
- [3] V. V. Teleshov, E. Ya. Kaputkin, A. P. Golovleva, N. P. Kosmacheva. Temperature ranges of phase transformation and mechanical properties of alloys of the Al–Cu–M –Ag system with various Cu: Mg rations, *Metal Sci.and Heat Treat.* 47 (2005) 139-144.
- [4] I.J. Polmear, M.J. Couper, Design and development of an experimental wrought aluminium alloy for use at elevated temperatures, *Metall. Trans. A* 19A (1988) 1027–1035.
- [5] S. P. Ringer, T. Sakurai, I. J. Polmear, Origins of hardening in aged Al-Cu-Mg-(Ag) alloys, *Acta Mater.* 45 (1997) 3731-3744.
- [6] M. Gazizov, R. Kaibyshev, Effect of over-aging on the microstructural evolution in an Al–Cu–Mg–Ag alloy during ECAP at 300°C, *Journal of Alloys and Comp.* 527 (2012) 163–175.
- [7] I.J. Polmear, *Light Alloys. From traditional alloys to nanocrystals*, third ed., Butterworth-Heinemann/Elsevier, UK, 2006.
- [8] M. Vural, J. Caro, Experimental analysis and constitutive modeling for the newly developed 2139-T8 alloy, *Mater. Sci. & Eng. A* 520 (2009) 56–65.
- [9] J. Pilling and N. Ridley: *Superplasticity in Crystalline Solids*, The Institute of Metals, London, 1989, p. 214.
- [10] Y. Brechet, Y. Estrin, On the influence of precipitation on the Portevin-Le Chatelier effect, *Acta Metall. Mater.* Vol. 43 (1995) 955–963.
- [11] ASM Handbook 12 (1987) 857.